OPTIMIZATION OF DESIGN OF EXHAUST SYSTEM OF AN IC-ENGINE FOR MINIMUM EMMISIONS OF CO & NOX

K. S. UMESH[1], V. K. PRAVIN[2] & K. RAJAGOPAL[3]

[1]Department of Mechanical Engineering, Thadomal Shahani Engineering College, Mumbai, Maharashtra, India

[2]Department of Mechanical Engineering, P. D. A. College of Engineering, Gulbarga, Karnataka, India

[3]Former Vice Chancellor, JNT University, Hyderabad, Andhra Pradesh, India

ABSTRACT

Exhaust gas travels through Cylinder head and exhaust manifold, a turbocharger to increase engine power, a catalytic converter to reduce air pollution and noise reducer such as muffler. Inside the manifolds the exhaust gases coming out of multiple cylinders are collected and then directed through towards catalytic converters. Catalytic converters are generally fitted in series with the exhaust pipe of almost all vehicles. Inside the Catalytic converter Harmful gases like Co, No etc. are converted into CO_2, N_2 etc. respectively. They oxidize carbon monoxide (CO) to carbon dioxide (CO2), and reduce nitrogen oxides (NOx) into nitrogen and water vapors. This work is based on combination of experimental and computational investigations to optimize the design of exhaust system from emission point of view. The aim of this work is to optimize design of exhaust manifold in order to improve filtration efficiency of catalytic converter with MC-2 configuration using Cu as a catalyst. Amongst various constituents of exhaust gas, CO and NO are most dangerous pollutants from Global warming point of view. Thus this particular work is concentrated on analyzing filtration efficiency for these two pollutants.

KEYWORDS: CFX, CATIA V5, Gambit 2.2, DETCHEM, Fluent 6.2, SBCE, SBCER, LBCE, LBCER, SBSE, SBSER, LBSE, LBSER, Relative A: F Ratio (λ)

INTRODUCTION

Conversion efficiency of catalytic converter is the measure of amount of CO oxidized to CO_2 or Amount of NOx reduced to N_2.

Kulal et.al (2012) analyzed three different configurations of catalytic converters viz. MC-1, MC-2 and MC-3 for flow characters like velocity distribution & pressure drop to optimize the design for minimum particulate matter in the exhaust. Kulal et.al (2013) analyzed by CFD analysis effect of manifold geometry on emissions. Kulal et.al (2014) analyzed performance of catalytic converter with MC-1, MC-2 & MC-3 configuration with metallic copper as catalyst and proved that catalytic converters of MC-2 configuration gives best filtration efficiency compared to others for harmful pollutants like NO_x and CO. Kulal et.al (2014) analyzed performance of catalytic converter with MC-2 configuration with various metal catalysts and proved that copper can prove to be an effective long term replacement to precious & rare earth metals like platinum, palladium and rhodium.

This particular work is extended discussion of these 4 previously presented research papers presented by us (Refer: **Reference**: 13, 15, 16 & 19).

METHODOLOGY

This paper deals with the study of fluid flow inside the entire exhaust system starting through exhaust manifold; then through catalytic converter and the study of temperature distribution and chemical reaction in catalytic converter. CATIA V5 R-15 was used for geometric modeling of catalytic converter. Discretization was done with Gambit 2.2 and flow was analyzed with fluent. Detchem was used for chemical analysis.

In comparison to the Navier-Stokes equations, the diffusion terms along the direction of convection are neglected. This model has been proven useful for higher flow velocities, as they are expected in this application.

We have considered two chemical reactions. The oxidation reaction of CO and hydrocarbons and reduction reaction of NO were considered. The hydrocarbons were represented by propylene, which is easily oxidized hydrocarbon, constitute about 80% of the total hydrocarbons found in the typical exhaust gas. The chemical reactions are:

- **Oxidation of Carbon Monoxide**

$$2CO + O_2 \rightarrow 2CO_2 \tag{1}$$
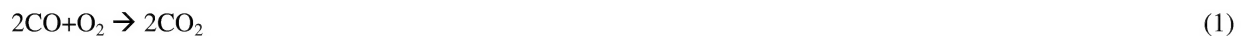
- **Oxidation of Hydro Carbon**

$$2C_3H_6 + 9O_2 \rightarrow 3CO_2 + 6H_2O \tag{2}$$

- **Reduction of Nitrous Oxide**

$$CO + NO \rightarrow CO2 + \tfrac{1}{2} N2 \tag{3}$$

MODEL DESCRIPTION

We have considered 8 different models of exhaust manifold for this particular research.

The eight models considered for this work are

- Short Bend Center Exit (SBCE)

- Short Bend Side Exit (SBSE)

- Long Bend Center Exit (LBCE)

- Long Bend Side Exit (LBSE)

- Short Bend Center Exit with Reducer (SBCER)

- Short Bend Side Exit with Reducer (SBSER)

- Long Bend Center Exit with Reducer (LBCER)

- Long Bend Side Exit with Reducer (LBSER)

The Header length for all manifold was kept same i.e. 335 mm. The longer bend models had bend radius of 100 mm whereas shorter bend models had bend radius of 48 mm.
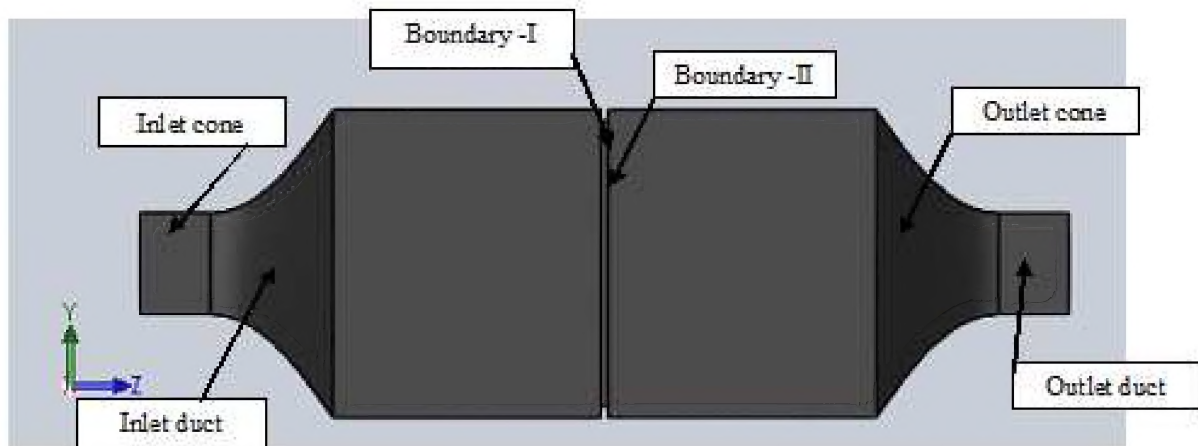
Figure 1: Catalytic Converter

For the simulations a commercially available three-way catalytic converter with a rectangular cross-section was assumed. The specifications of the substrate, the coating and the canning are listed in following tables:

Table 1: Model Description

Property	1St Compartment	2nd Compartment
Cell Density (Cells/ Inch^2)	144	324
Hydraulic Diameter (mm)	0.51	0.41
Uncoated Wall Thickness (mm)	8	6
Wash coat Thickness (µm)	20	20
Porosity (%)	57.7	50.8

Substrate: Knitted Steel Wire

Coating: Copper (50gm/ft^3)

Inlet Dimensions: 38 X 56 mm

Cross Section: 176 X 110 mm

Length of One Section: 153 mm
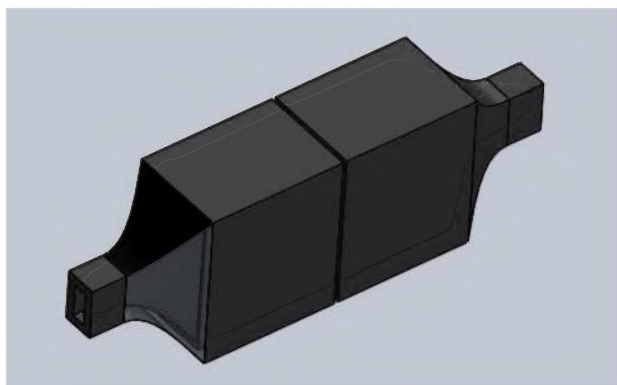
Figure 2: 3-D View of Catalytic Converter   **Figure 3: Side View of Grid**
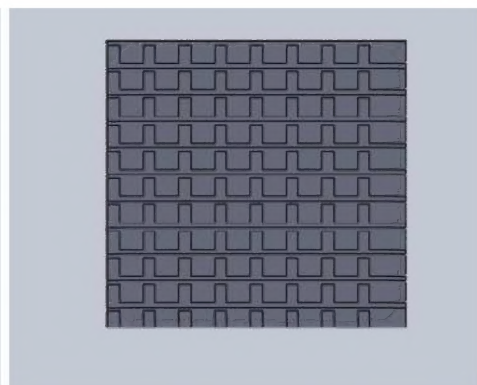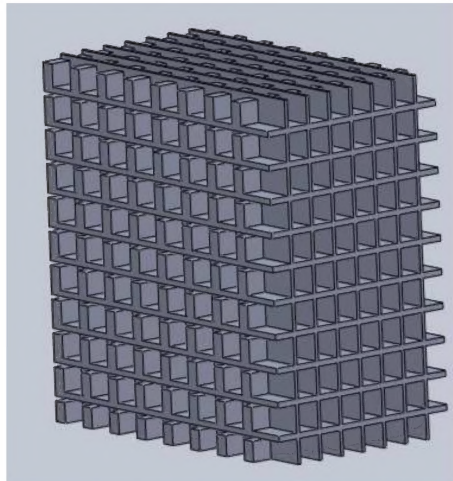
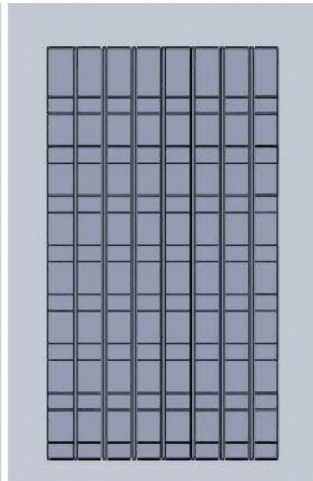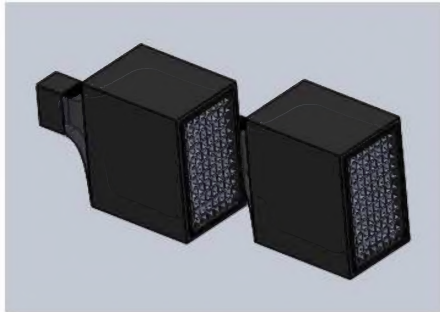**Figure 4: 3-D View of Grid   Figure 5: Top View of Grid**

Figure 6: 3-D View of Two Compartments   Figure 7: Assembled Compartment
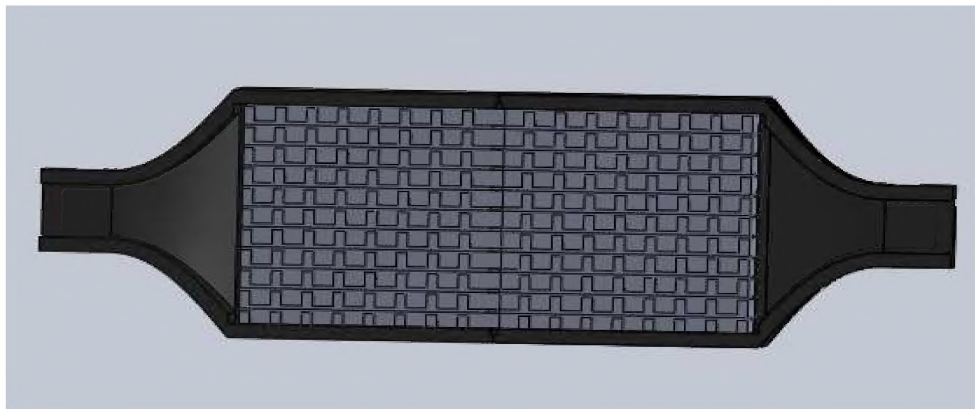

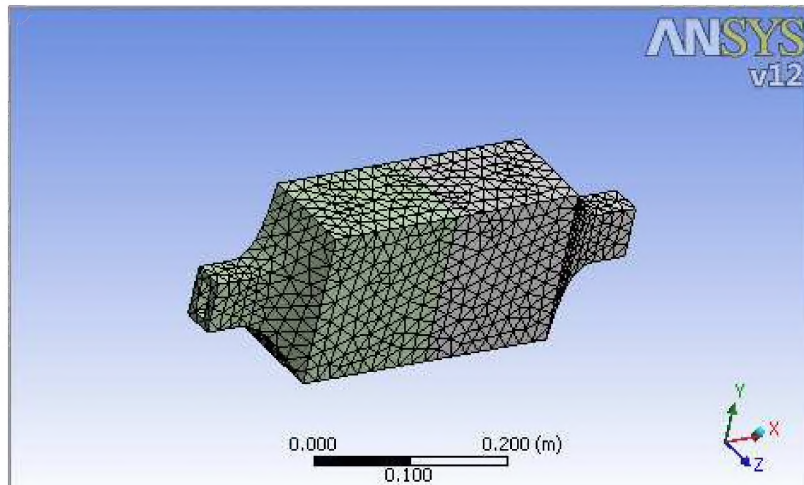**Figure 8: Path of Exhaust Gas through Catalytic Converter**
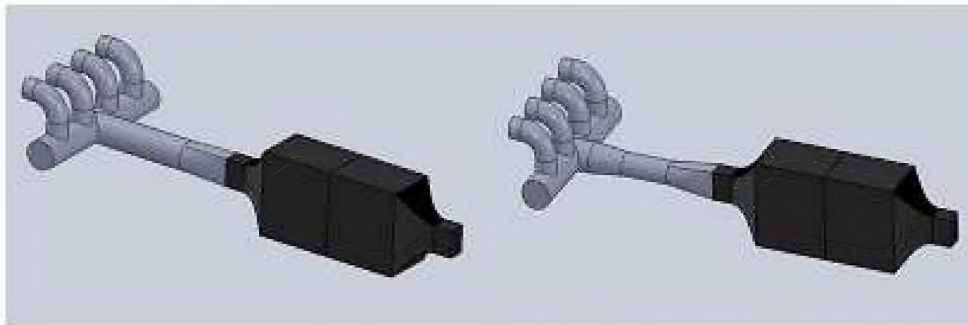
Figure 9: Meshed Model

The eight models are as follows:

Figure 10: SBCE & SBCER
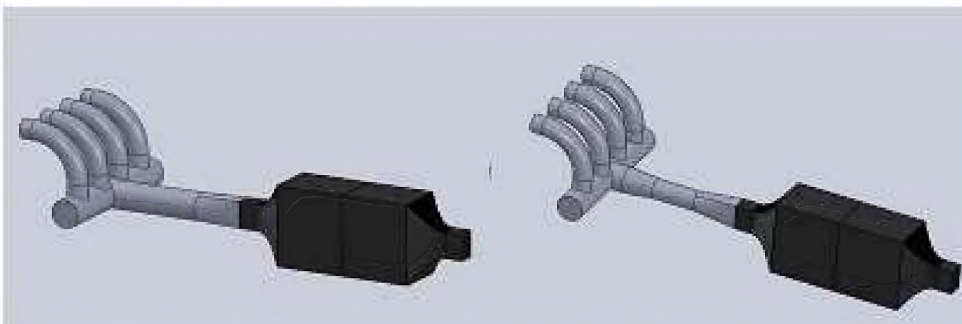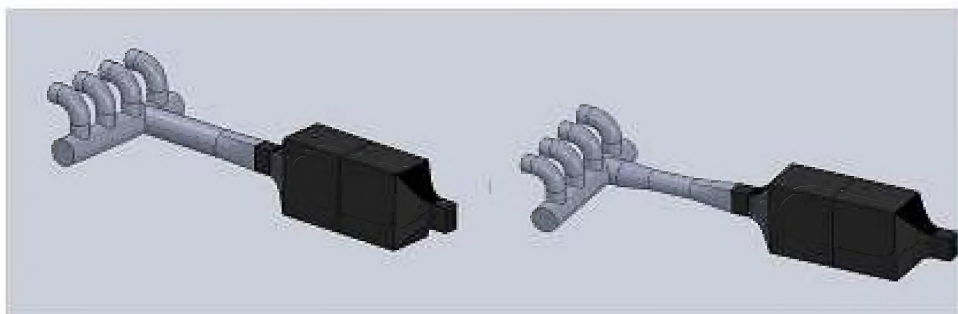

Figure 11: LBCE & LBCER
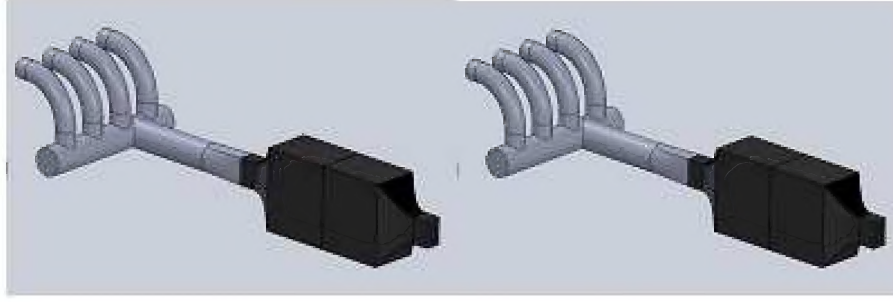

Figure 12: SBCE & SBCER

Figure 13: LBCE & LBCER

MATHEMATICAL AND NUMERICAL MODEL

Numerical Model for the simulation was developed using below equations. Flow was transient and unsteady.

The equations to be solved are:

- **Conservation of Total Mass**

$$\frac{\partial(r\rho u)}{\partial z} + \frac{\partial(r\rho v)}{\partial r} = 0$$

(1)

- **Conservation of Species Mass**

$$\frac{\partial(r\rho u Y_i)}{\partial z} + \frac{\partial(r\rho v Y_i)}{\partial r} = -\frac{\partial}{\partial r}(r j_i)$$

(2)

- **Conservation of Axial Momentum**

$$\frac{\partial(r\rho uu)}{\partial z} + \frac{\partial(r\rho vu)}{\partial r} = -r\frac{\partial p}{\partial z} + \frac{\partial}{\partial r}\left(\mu r \frac{\partial u}{\partial r}\right)$$

(3)

- **Conservation of Enthalpy**

$$ru\frac{\partial p}{\partial z} + \frac{\partial}{\partial r}\left(\lambda r \frac{\partial T}{\partial r}\right) - \frac{\partial}{\partial r}\left(\sum_i r j_i h_i\right)$$

(4)

Despite the actual shape of the channels, a cylindrical model is used in order to reduce the numerical complexity.

Catalytic reactions at the surface are taken into account in terms of the diffusive mean flux j_i at the gas phase wash coat interface in Equation 2.

$$j_{i,surf} = \eta F_{cat/geo} M_i \dot{s}_i$$

(5)

$$\dot{s}_i = \sum_{k=1}^{K_s} \nu_{ik} k_{fk} \prod_{j=1}^{N_g+N_s} c_j^{\nu'_{jk}}$$

(6)

$$k_{fk} = A_k T^{\beta_k} \exp\left[\frac{-E_{ak}}{RT}\right] f_k\left(\Theta_1, \ldots, \Theta_{N_s}\right)$$

(7)

$$f_k\left(\Theta_1, \ldots, \Theta_{N_s}\right) = \prod_{i=1}^{N_s} \Theta_i^{\mu_{ik}} \exp\left[\frac{\varepsilon_{ik} \Theta_i}{RT}\right]$$

(8)

The boundary-layer equations can be solved in a single sweep of integration along the axial direction by a method-of-lines procedure using an adaptive integration step size. The radial derivatives are discretized using a finite-volume method. The resulting differential-algebraic equation system is integrated using the semi-implicit extrapolation solver LIMEX.

Using this steady-state channel model, a transient simulation of the thermal behavior of the entire catalytic converter is performed by DETCHEM$_{MONOLITH}$. The solid's temperature field is described by a three-dimensional conservation equation:

$$\frac{\partial T_{monolith}}{\partial t} = \nabla^2\left(\frac{\lambda T_{monolith}}{\rho c_p}\right) + \frac{q}{\rho c_p}$$

(9)

$$q = -\sigma \cdot 2\pi r \lambda \left.\frac{\partial T_{gas}}{\partial r}\right|_{surface}$$

(10)

Boundary Conditions

The simulation and analysis was carried out at different exhaust temperatures ranging between 250 degree Celsius & 1000 degree Celsius. Also we considered 3-different A: F ratios:

Table 2: A: F Ratio

Rich Mixture	Relative A:F Ratio (λ_{OX}) 0.5
Nearly Stochiometric Mixture	Relative A:F ratio (λ_{OX}) 0.9
Lean Mixture	Relative A:F ratio (λ_{OX} 1.5

Table 3: Applied Boundary Conditions

Entity	Zone	Zone Type
mass flow inlet	boundary	Inlet
pressure outlet	boundary	Outlet
boundary 1	boundary	wall-reduction
boundary 2	boundary	wall-oxidation

The exhaust gas mass composition was determined experimentally for 3 A: F ratios. The engine specifications were as follows:

Table 4: Engine Specifications

Engine	4 Stroke 4 Cylinder SI Engine
Make	Maruti-Suzuki Wagon-R
Calorific Value of Fuel (Gasoline)	45208 KJ/Kg-K
Specific Gravity of Fuel	0.7
Bore and Stroke	69.05mm x 73.40mm
Swept Volume	1100cc
Compression Ratio	7.2:1
Dynamometer Constant	2000
Diameter of Orifice	29mm
Coefficient of Discharge	0.65

The average Composition of exhaust gas was found out experimentally at various air fuel ratios by flue gas analysis. The air fuel ratio was varied and the proportion of various constituents of exhaust gas was calculated from that.

Table 5: Exhaust Gas Composition

	% CO	% NO_X	% CO_2	% H_2O	% HC	%N_2	% O_2	Others	Total
λ =1.5	0.01484	0.00170	8.406	18.126	0.754	71.814	0.844	0.03945	100
λ =0.9	0.01534	0.00167	7.762	18.158	0.776	71.986	0.87	0.43098	100
λ =0.5	0.01588	0.00155	7.808	18.078	0.926	71.924	0.79	0.45656	100

RESULTS

The exhaust gas composition provided composition of exhaust gas at the entry point of the model Table 5. Each of the eight models as discussed earlier consisted of 4 inlets and one outlet. The chemical reaction and flow taking place inside the entire exhaust system was simulated as discussed earlier. The outlet composition was evaluated a result of this simulation.

Once this result was obtained, the conversion efficiency of CO & NO was evaluated for each model.

$$\textbf{Conversion efficiency of "X"} = \frac{Inlet\ mass\ fraction\ of\ "X" - Outlet\ mass\ fraction\ of\ "X"}{Inlet\ Mass\ Fraction\ of\ X} \times 100$$

Thus similarly we carried out 24 simulations on each model by considering 8 simulations at 8 different exhaust temperature between 300 to 1000 ^{O}C for these simulations {At each of these eight temperatures; 3 simulations for 3 different A:F ratios Table 2}

Thus, after evaluating such conversion efficiencies for all simulations on all models which resulted in series of values; these obtained values were plotted on graphs shown below Taking 1 A:F ratio at time and plotting conversion efficiency VS exhaust temperature for all models resulting in below 6 plots (3 for 3 A:F ratios and such two sets for CO and NO_x respectively).
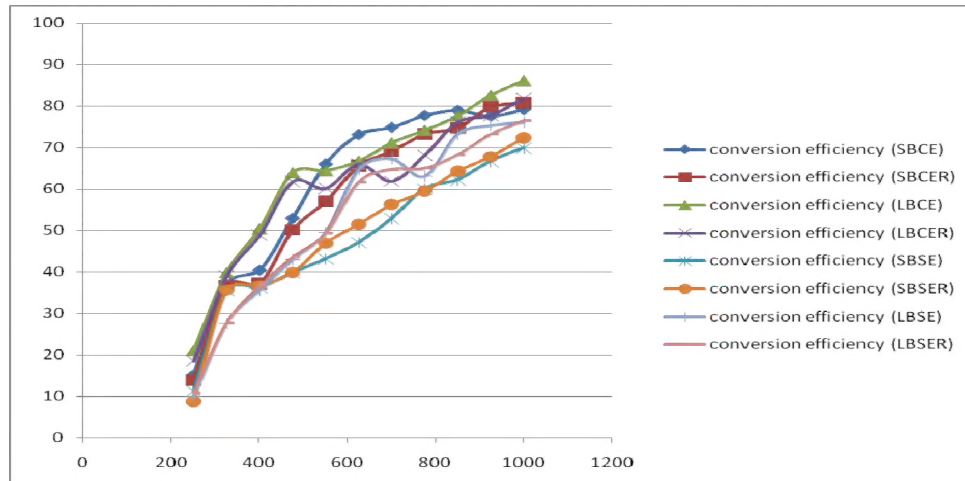
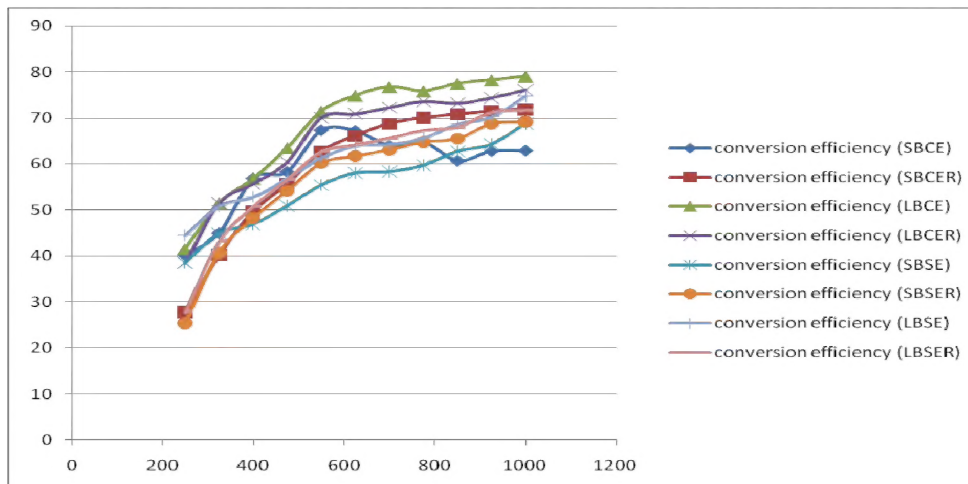**Figure 14: CO Conversion Efficiency vs Temperature for Different Models (λ =0.9)**

Figure 15: NO$_x$ Conversion Efficiency vs Temperature for Different Models (λ =0.9)

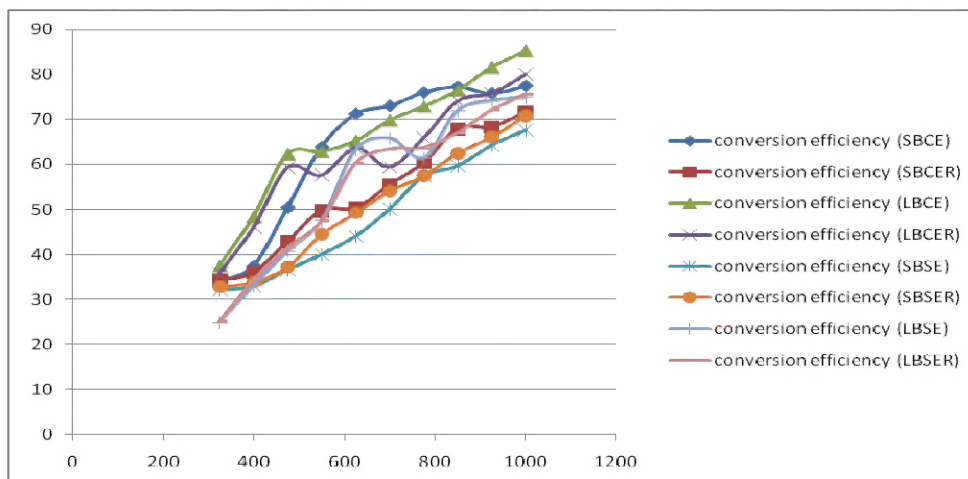**Figure 16: CO Conversion Efficiency vs Temperature for Different Models** (λ =1.5)
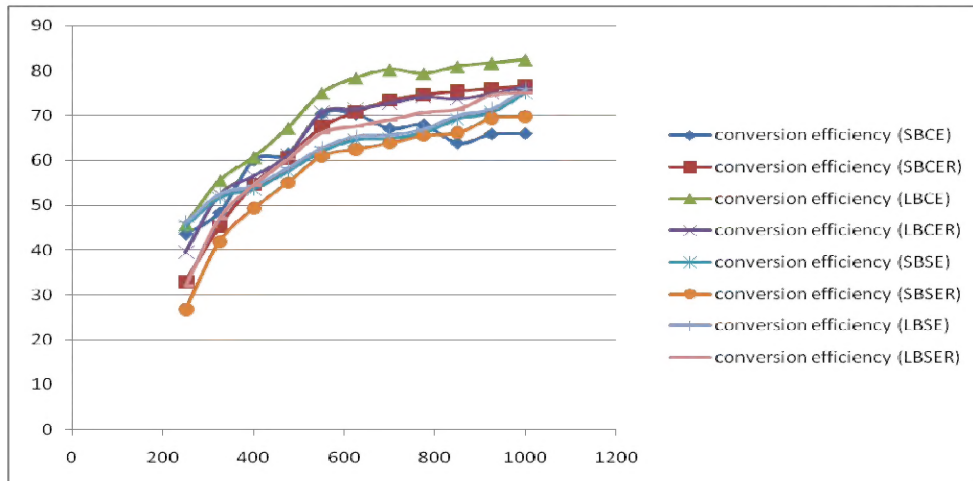
Figure 17: NOₓ Conversion Efficiency vs Temperature for Different Models ($\lambda =1.5$)
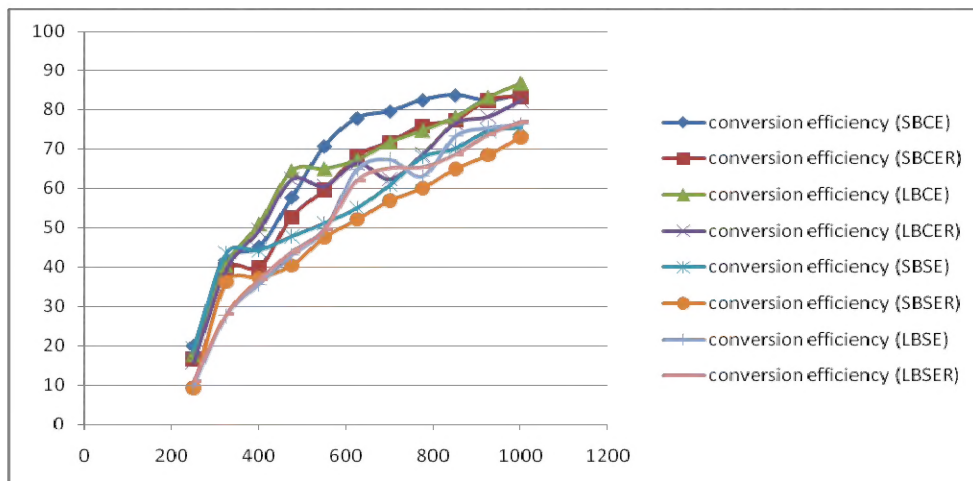

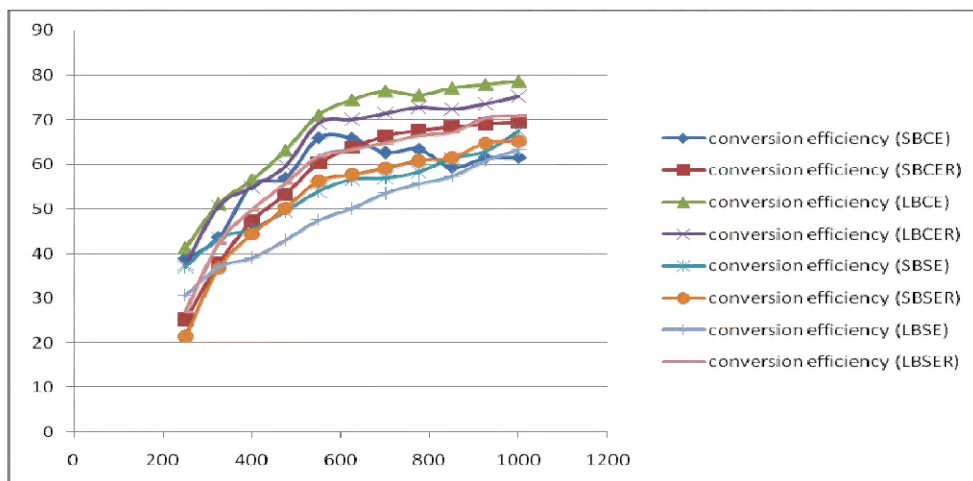**Figure 18: CO Conversion Efficiency vs Temperature for Different Models** ($\lambda =0.5$)

Figure 19: NOₓ Conversion Efficiency vs Temperature for Different Models ($\lambda =0.5$)

CONCLUSIONS

From Figure: 14-19 it can be easily concluded that **conversion Efficiency** for NO_x was found to be **highest** with **LBCE** exhaust manifold. Whereas **conversion Efficiency** for CO was found to be **highest** with **LBCE & SBCE** exhaust manifold.

K.S. Umesh, V.K. Pravin & K. Rajagopal in their "CFD Analysis of Exhaust Manifold of Multi-cylinder SI Engine to Determine Optimal Geometry for Reducing Emissions" (Refer: **References:** 16) predicted that LBCE is indeed a best model from emission point of view by analysis of exhaust velocity and back pressure contours obtained as a result of flow simulations through the same eight models under discussion.

Thus our work justifies those claims by confirming the results. Thus we conclude that **LBCE** is indeed best design from emission point of view amongst models under discussion

Also another fact that was observed from Figure 14-19:

$$\sum_{n=1}^{4} \text{Area under conversion efficiency curve for all basic models (i. e. with reducer)} < \sum_{n=1}^{4} \text{Area under conversion efficiency curve for all modified models (i. e. without reducer)}$$

Please note that we are referring SBCE. SBCE, LBCE and LBSE as basic models and same 4 models attached with reducer as

Modified models (i.e. SBCER, SBSER, LBCER, LBSER).

Thus we can conclude that addition of reducer reduces conversion efficiency for models under discussion.

Above stated conclusions and Figure 14-19 indicate that conversion efficiency of the various pollutants is dependent upon symmetry of the design in some or the other way.

Thus to find out the exact relationship between the symmetry of the design and conversion efficiency of various we have evaluated **design symmetry** of each design in terms of **mean deviation of the lengths of path travelled by exhaust gas stream coming out of each cylinder up to outlet of exhaust manifold**

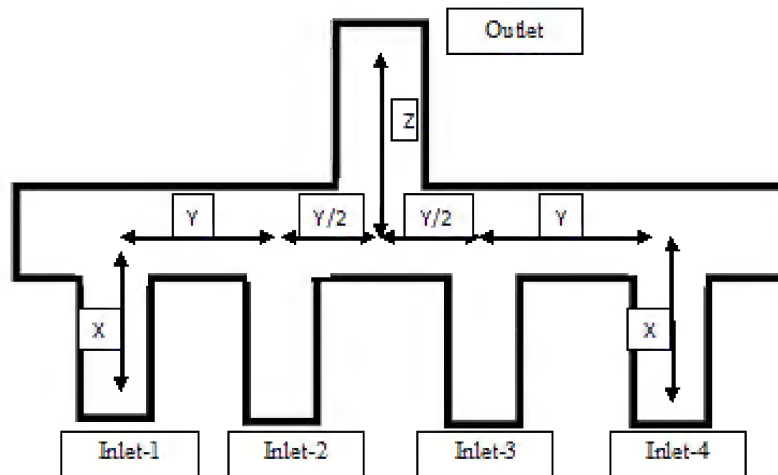**For Example**

Consider a SBCE model shown below:

Figure 20: SBCE Exhaust Manifold Block Diagram

Let,

L_i = Path travelled by exhaust gas from inlet "i" to Outlet

Thus for above SBCE model under consideration

L1= X+ Y + (Y/2) + Z

(Refer figure 27 for further information regarding these Dimensions)

L1 = L3= $\{(\frac{\pi}{2})$ x 48$\}$ + 85 + 42.5 + 220 (Dimensions are in mm)

L2 = L4= $\{(\frac{\pi}{2})$ x 48$\}$ + 42.5 + 220 (Dimensions are in mm)

Lavg = $\dfrac{\sum_{n=1}^{4} Li}{4}$

ΔL_i = $\sqrt[2]{(Li - Lavg)}$ (Where "i" = 1 to 4)

ΔL = $\dfrac{\sum_{n=1}^{4} \Delta Li}{4}$

This "ΔL" can be treated as measurement of symmetry of exhaust manifold. We have evaluated design symmetry of all the models under consideration as follows:

Table 6: Evaluation of Design Symmetry (ΔL)

Model	L1	L2	L3	L4	Lavg	ΔL
SBCE	422.86	337.86	337.86	422.86	380.36	0.223472
SBCER	422.86	337.86	337.86	422.86	380.36	0.223472
LBCE	504.5	419.5	341	504.5	442.375	0.307624
LBCER	504.5	419.5	341	504.5	442.375	0.307624
SBSE	337.86	337.86	385.18	507.86	392.19	0.354523
SBSER	337.86	337.86	385.18	507.86	392.19	0.354523
LBSE	419.5	419.5	504.5	589.5	483.25	0.291685
LBSER	419.5	419.5	504.5	589.5	483.25	0.291685

One can easily observe that all the basic and corresponding modified models have same design symmetry factor. Thus we have evaluated average conversion efficiency of those two models in below plots in which we have plotted variation of conversion efficiency with ΔL at various temperatures and A:F ratios. (One can note that these plots indicate same variation indicated by above plots; but instead on 8 curves we would be having only 4 curves per graph)

Conversion efficiency for models with "ΔL =X" = $\dfrac{\textit{Sum of Conversion efficiency for models with "}\Delta L = X\text{"}}{\textit{No of models with "}\Delta L = X\text{"}}$

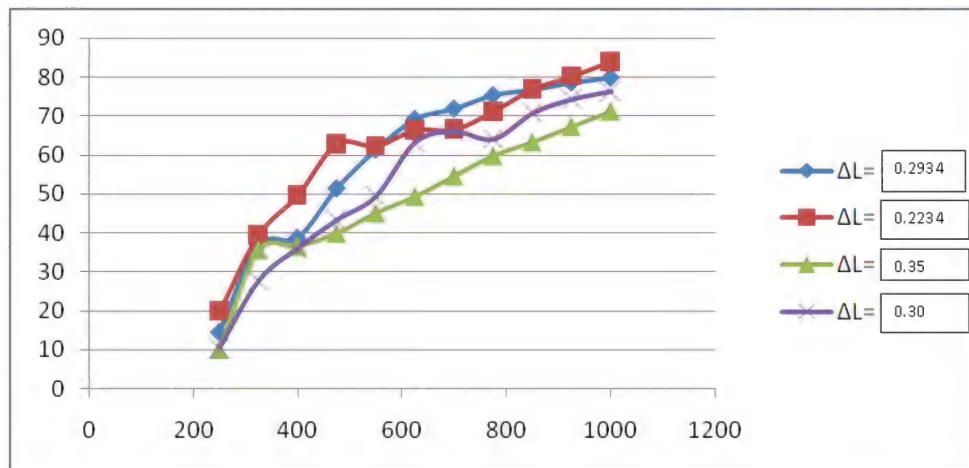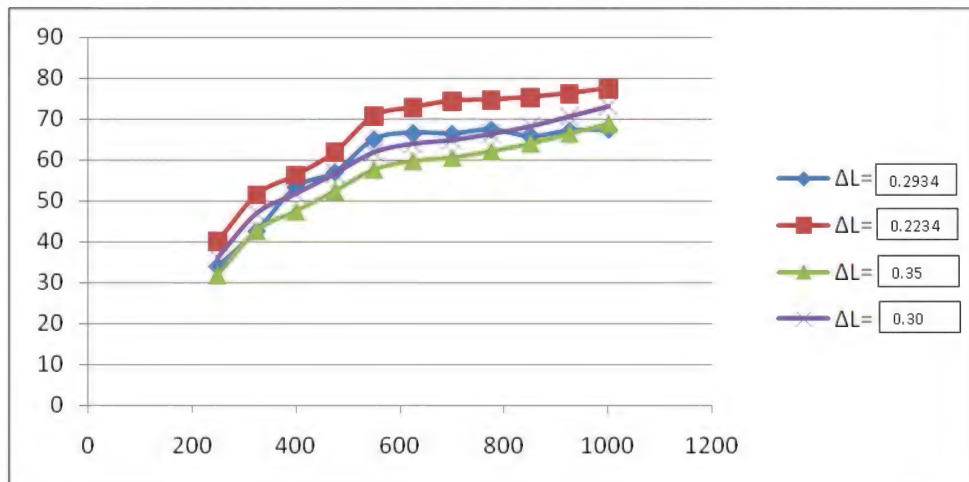**Figure 21: CO Conversion Efficiency vs Temperature for ΔL (λ =0.9)**

Figure 22: NO$_x$ Conversion Efficiency vs Temperature for ΔL (λ =0.9)

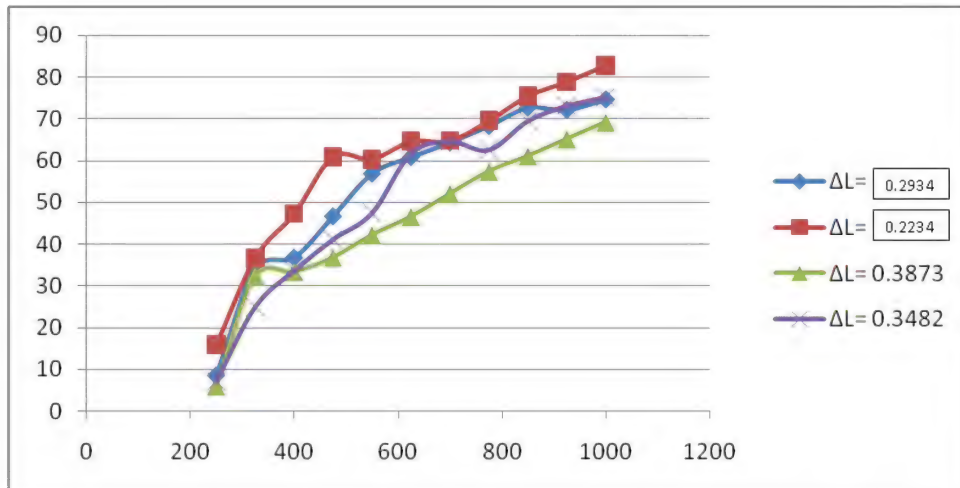**Figure 23: CO Conversion Efficiency vs Temperature for ΔL (λ =1.5)**
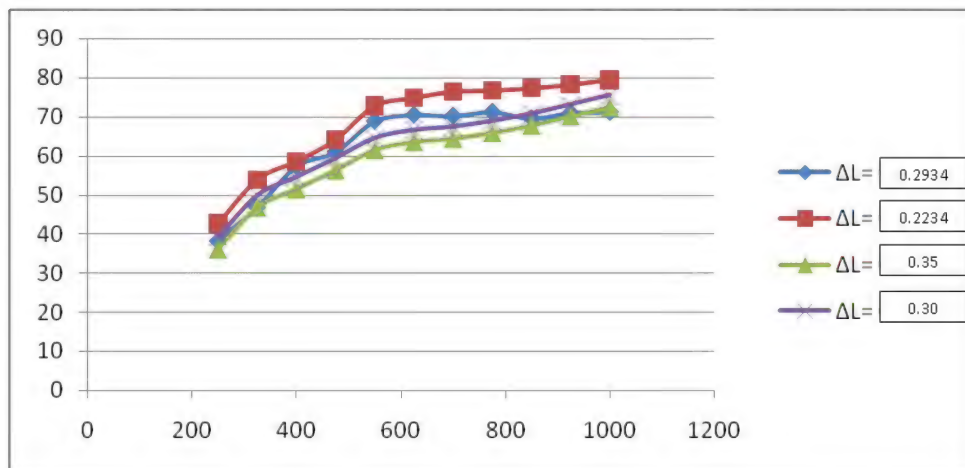

Figure 24: NO$_x$ Conversion Efficiency vs Temperature for ΔL (λ =1.5)
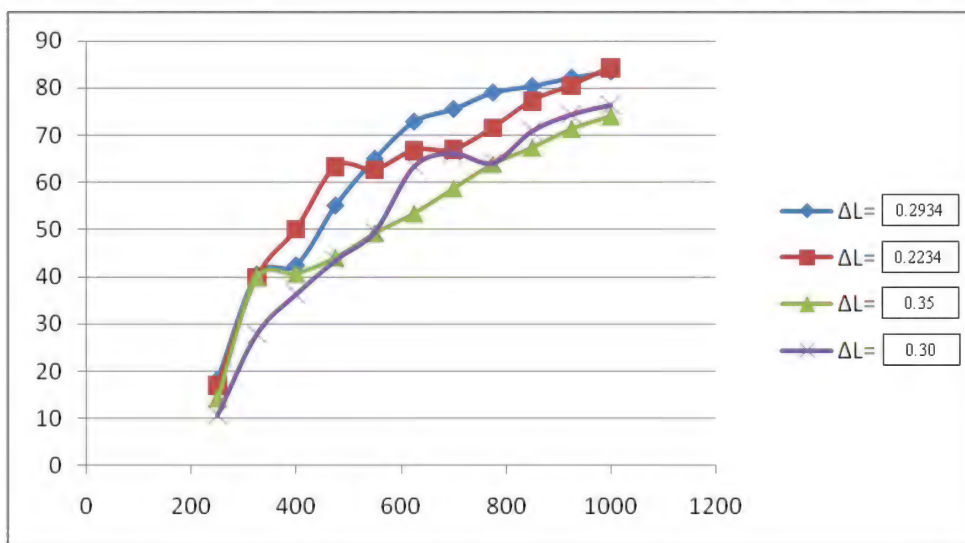

Figure 25: CO Conversion Efficiency vs Temperature for ΔL (λ =0.5)
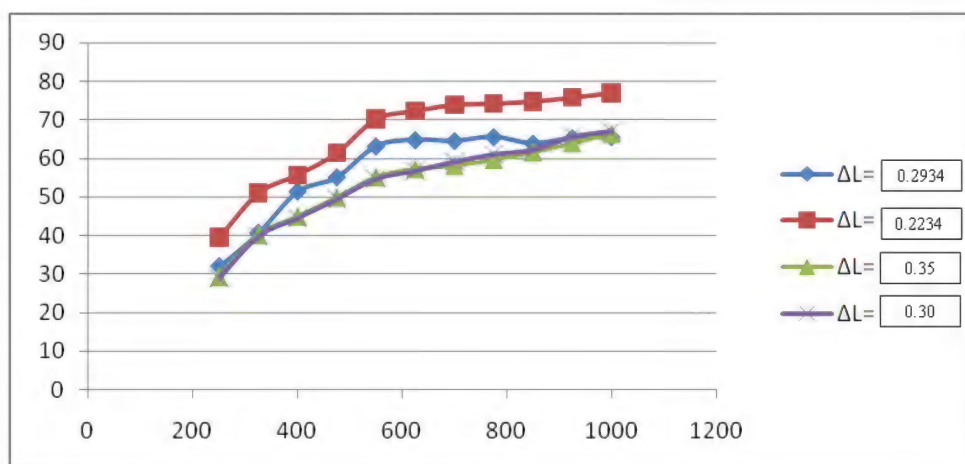
Figure 26: NO$_x$ Conversion Efficiency vs Temperature for ΔL (λ =0.5)

From above plots (Figure 21-26) we can conclude that both CO Conversion Efficiency and NOx Conversion efficiency varies inversely as ΔL.

Hence the inference is; for higher conversion efficiency for both Co and NO$_x$ the value of ΔL must be close to zero as far as possible.

REFERENCES

1. PL. S. Muthaiah, Dr. M. Senthil Kumar, Dr. S. Sendilvelan "CFD Analysis of catalytic converter to reduce particulate matter and achieve limited back pressure in diesel engine" Global journal of researches in engineering – A: Classification(FOR) 091304,091399, vol.10 Issue 5 (Ver1.0) October 2010.

2. P. R. Kamble and S.S. Ingle "Copper Plate Catalytic Converter: An Emission Control Technique" SAE Number 2008-28-0104.

3. M.B. Beardsley et al., (1999). "Thermal Barrier Coatings for Low Emission", High Efficiency Diesel Engine Applications" SAE Technical Paper 1999-01-2255.

4. Eberhard Jacob, Rheinhard Lammermann, Andreas Pappenherimer, and Diether Rothe "Exhaust Gas After treatment System for Euro 4" Heavy Duty Engines – MTZ 6/2005.

5. Jacobs, T., Chatterjee, S., Conway, R., Walker, A., Kramer, J. And Mueller- Haas, K. "Development of a Partial Filter Technology for Hdd Retrofit" Sae Technical Paper 2006-01-0213.

6. C. Lahousse, B. Kern,H. Hadrane and L. Faillon " Backpressure Characteristics of Modern Three-way Catalysts, Benefit on Engine Performance" SAE Paper No. 2006-01-1062, 2006 SAE World Congress, Detroit, Michigan, April 3-6,

7. 2006.Zbigniew Zmudka, Adam Ciesiolkiewicz "Comprehensive approach to the work of Catalysts in Engine exhaust system", Journal of KONES I.C. Engine, Vol. 11, pp. 368-375

8. A.K.M. Mohiuddin and Muhammad Nurhafez "Experimental analysis and comparison of performance characteristics of catalytic converters including simulation" International Journal of Mechanical and Materials Engineering (IJMME), vol. 2 (2007), No. 1, 1-7

9. He, L.; Yu, X.-M.; Li, G.-L.; Xu, N. 2012. Dynamic Response of a Three-Way Catalytic Converter, Energy Procedia, Volume 17 Part A, pp. 547-554, ISSN 1876-6102.

10. V.K. Pravin, K.S. Umesh, K. Rajagopal, P.H. Veena "Numerical Investigation of Various Models of Catalytic Converters in Diesel Engine to Reduce Particulate Matter and Achieve Limited Back Pressure" International Journal of Fluids Engineering. ISSN 0974-3138 Volume 4, Number 2 (2012), pp. 75-88.

11. K.S. Umesh,V.K. Pravin,, K. Rajagopal, P.H. Veena "Optimum solution of catalytic converter with filtration efficiency of trap system by developing limited backpressure in diesel engine" International Research Journal of Engineering Science, Technology and Innovation (IRJESTI) Vol. 1(6) pp. 152-160, September 2012

12. Robert H. Perry and Don W. Green "Perry's Chemical Engineering Handbook", Seventh edition, McGraw Hill International Editions, Chemical Engineering Series, 1997

13. K.S. Umesh, V.K. Pravin,, K. Rajagopal "Analysis of performance of various models of copper based catalytic converters by C.F.D. techniques" International Journal of Automobile Engineering Research and Development (IJAuERD) ISSN(P): 2277-4785; ISSN(E): 2278–9413, vol. 4, Issue 1, Feb 2014, 27-40

14. K.S. Umesh, V.K. Pravin,, K. Rajagopal "Analysis of performance of various metal catalysts used in catalytic converters with MC-2 configuration by C.F.D. techniques" International Journal of Automobile Engineering Research and Development (IJAuERD) ISSN(P): 2277-4785; ISSN(E): 2278–9413, vol. 4, Issue 1, Feb 2014, 41-54

15. K.S. Umesh, V.K. Pravin, K. Rajagopal "Numerical Investigation of Exhaust Manifold Designs by Evaluation of Performance Score to select Best Possible Geometry Based on the Application" published in international conference on Advances in Mechanical Engineering (AME) in December 2013.

16. K.S. Umesh, V. K. Pravin, K. Rajagopal "CFD Analysis Of Exhaust Manifold Of Multi-cylinder SI Engine To Determine Optimal Geometry For Reducing Emissions" published in International Journal of Automobile Engineering Research and Development ISSN (Online): 2278-9413, ISSN(Print): 2277-4785, Impact Factor(JCC): 4.8725 vol. 3, Issue 4, Oct 2013, 45-56

17. K.S. Umesh, V.K. Pravin, K. Rajagopal "Experimental Investigation of Various Exhaust Manifold Designs and Comparison of Engine Performance Parameters for These to Determine Optimal Exhaust Manifold Design for Various Applications" published in international conference on Advances in Mechanical Engineering (AME) in December 2013.

18. K.S. Umesh, V.K. Pravin, K. Rajagopal "Experimental Analysis of Dependence of volumetric efficiency of Multi-cylinder SI Engine on manifold geometry and Verification of Results Obtained through Analysis at particular Speed for different Speed Condition "published by International Journal of Engineering Science and Research. (Ref No: -Volume 04, Article 08283; August 2013)

19. K.S. Umesh, V. K. Pravin, K. Rajagopal "Experimental Analysis of Optimal Geometry for Exhaust Manifold of Multi cylinder SI Engine for Optimum Performance" published by International Journal of Automobile Engineering Research and Development, ISSN(Online): 2278-9413, ISSN(Print): 2277-4785, Impact Factor(JCC): 4.8725 vol. 3, Issue 4, Oct 2013, 11-22

NOTATIONS

- c_i Concentration
- cp Specific Heat
- fk Dependency Function
- hi Enthalpy of Species i
- h Enthalpy of the Mixture
- p Pressure
- q Heat Source term
- ji Diffusive Flux Including Surface Flux
- kfk Reaction Rate
- r Radial Spatial Coordinate
- A Face Area
- Ak Pre-Exponential Factor
- Eak Activation Energy
- $Fcat/geo$ Ratio of Catalytic to Geometric Surface Area
- Ks Number of Surface Reactions
- Mi Molar Mass
- Ng Number of Gas-Phase Species
- Ns Number of Surface Species
- R Gas Constant
- T Temperature
- λ_{OX} Relative A:F Ratio
- T Time
- u Axial Velocity
- v Radial Velocity
- w Normal Velocity
- w Mean Normal Velocity
- Yi Mass Fraction of Species i

- z Axial Spatial Coordinate

- βk Temperature Exponent

- εik Coverage Dependent Change of Activation Energy

- η Wash Coat Effectiveness Factor

- λ Thermal Conductivity

- γ Uniformity Index

- μ Viscosity

- μik Coverage Dependent Change of Reaction Order

- νik Stoichiometric Coefficients

- ρ Density

- σ Channel Density

- Θi Surface Coverage

APPENDICES
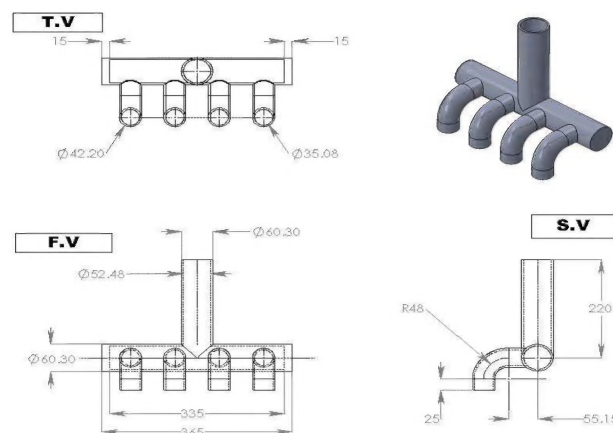
Figure 27: SBCE
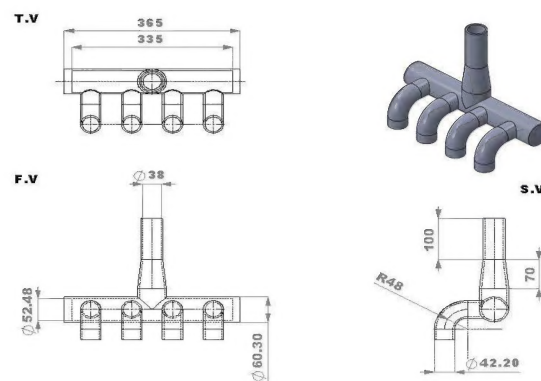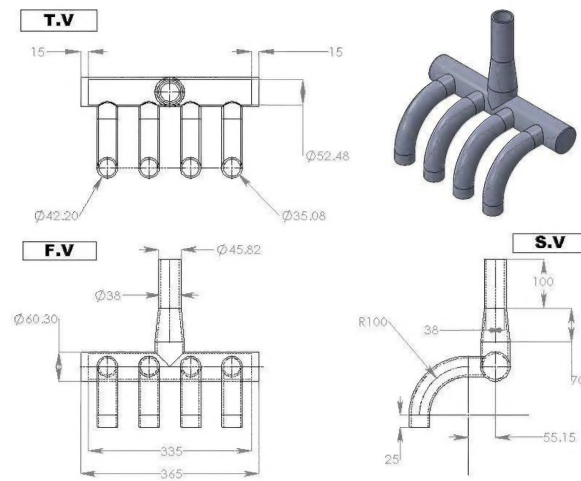

Figure 28: SBCER
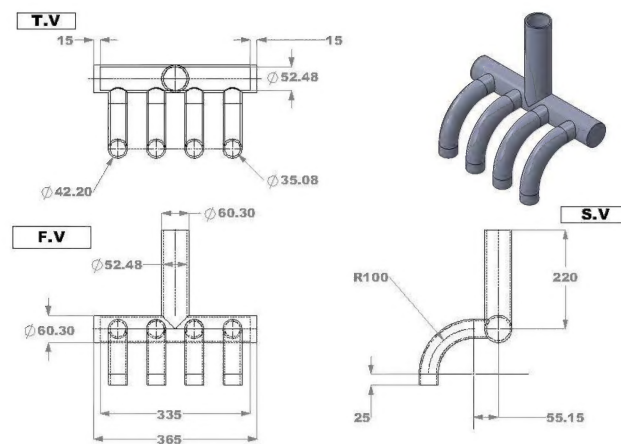
Figure 29: LBCE
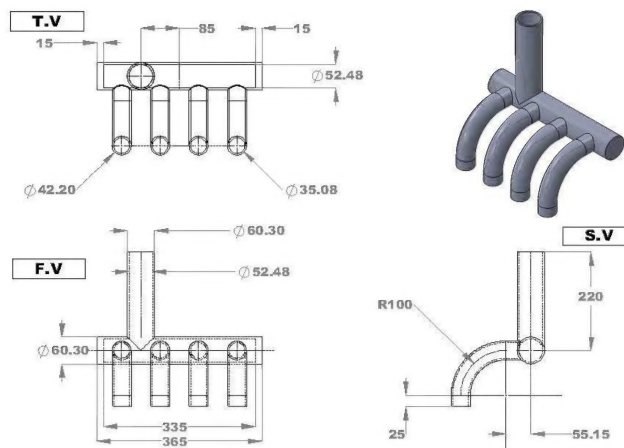

Figure 30: LBCER
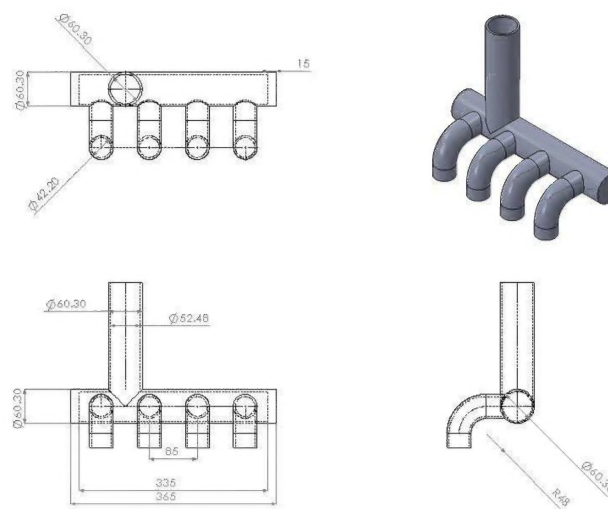
Figure 31: SBSE
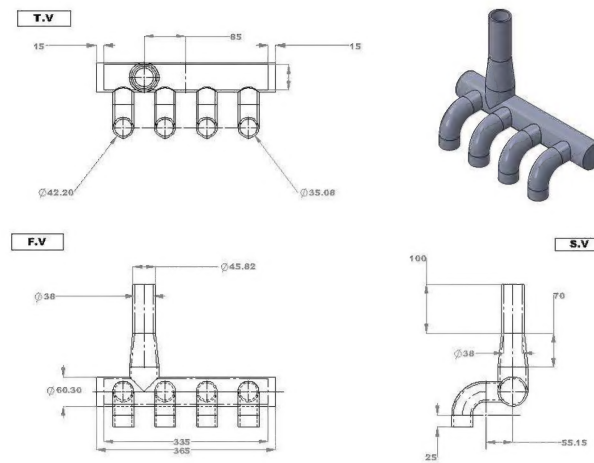
Figure 32: SBSER

Figure 33: LBSE

Figure 34: LBSER